

COLD MOLECULAR GAS AND NUCLEAR ACTIVITY IN RADIO GALAXIES.

Linking properties on macro and micro scales.

Eleonora Torresi (INAF-OAS, Bologna), **Paola Grandi** (INAF-OAS, Bologna) & **Viviana Casasola** (INAF-IRA, Bologna)
+ other collaborators

CONTEXT

In this work, we study the amount of cold molecular gas (CO) of a sample of radio galaxies representative of the four radio (FR I/FR II) and optical (HERG/LERG) classes in which they are divided. **The primary goal is to search for the main ingredient(s) that explain the observed variety of radio galaxies, particularly the existence of cross-populations.** Previous results (M20) suggested that FR II-LERG could be evolving sources experiencing a switch of the accretion regime from efficient to inefficient (evolutive scenario), or they could represent a separate class of inefficiently accreting objects.

To verify the evolutive scenario, we here concentrate on CO emission lines since they represent the best tracer of the molecular ISM, considered a fuel for the AGN activity. If there is a difference in the amount of cold molecular gas available for feeding the black hole, this difference could explain the different accretion rates measured for these sources.

Radio galaxies are classified as **FR I** or **FR II** based on their radio morphology (FR74) and as Low-Excitation Radio Galaxies (**LERG**) or High-Excitation Radio Galaxies (**HERG**) based on the optical emission lines in the Narrow Line Region (L94, JR97, B10). The latter classification reflects the accretion system in the central engine, which ionizes the gas in the NLR.

Therefore, LERG are generally powered by hot radiatively inefficient accretion flows (ADAF), while HERG accrete through a cold radiatively efficient Shakura-Sunyaev disk. FR II are generally associated with HERG (**FR II-HERG**), and FR I with LERG (**FR I-LERG**). This almost one-to-one correspondence points towards a direct link between the accretion mode and the plasma ejection (e.g., GC01).

However, there exists a non-negligible part of these sources not obeying the abovementioned one-to-one correspondence (Fig. 1): i) low radio power FR I with radiatively efficient accretion disks, i.e., **FRI-HERG**, and ii) powerful FR II radio sources hosting an inefficient hot thick flow, i.e., **FR II-LERG**.

FR II-LERG: X-ray properties

M20 studied the X-ray properties of a complete sample of 3CR FR II-LERG at $z < 0.3$ to reconcile the co-existence of an inefficiently accreting engine and an extended FR II morphology, the signature of a powerful jet. This study showed that FR II-LERG have **intermediate X-ray properties in the pc/sub-pc scale.**

The moderate intrinsic column density ($N_{\text{HX}} \sim 10^{22} \text{ cm}^{-2}$) and Eddington-scaled X-ray luminosities between FR II-HERG and FRI-LERG suggest that **FR II-LERG could represent an evolutionary stage of classical FR II.** They accreted efficiently in the past, producing powerful jets, and recently switched off their nuclear activity because, for example, they have exhausted the cold gas fuel. Still, this information has not yet reached the extended radio structures..

THE CO SAMPLE

To further explore the evolutive scenario that emerged from the X-ray study, we started a project aimed at investigating the CO cold gas amount in a sample of radio galaxies, searching for a possible depletion in the cold gas fuel in FR II-LERG that could explain the intermediate accretion rate values.

We built a sample of nearly 70 radio galaxies in the Northern hemisphere for which at least a ^{12}CO observation was reported in the literature (our reference papers are OF10, E05, SR11, L01). The redshift of the sources ranges from $z=0.00183$ to $z=0.128$. Each source was already classified in the radio (FR I/FR II) and optical (HERG/LERG) bands. Fig. 2 shows the fraction of the four classes of radio galaxies in the studied sample. **FR II-LERG** represent a non-negligible portion of radio-loud sources. Therefore, in the following, we will focus on these sources as **key targets to investigate the mutual relationship between accretion and jet power, independent of radio or optical classification.**

Fig. 3 shows the molecular gas mass distribution according to the different types of radio galaxies, i.e., FR I-LERG, FR II-LERG, FR I-HERG, FR II-HERG and Compact-HERG.

As a preliminary result, we find that when considering the radio and optical classifications (i.e., separating the effects of the HERG/LERG and FR I/FR II differences, G13), there is not a statistically significant difference between the molecular gas masses of FR II-LERG and HERG. A Kolmogorov-Smirnov test applied to the two datasets returned a probability $P_{\text{KS}}=0.20$, implying that they are drawn from the same distribution. Even considering upper limits, a two sample tests univariate program (TWOST) in the ASURV package (FN85) gave a probability $P_{\text{TWOST}}=0.27$.

Although we are dealing with a small number of sources and are aware of a dependence of M_{H_2} on the redshift (Fig. 4), this result weakens the evolutive scenario invoked to explain FR II-LERG sources.

Interestingly, B19 found a similar result by studying the warm ionized phase of the ISM with the MUSE spectrograph: the FR II-LERG and HERG of their sample show similar gas reservoirs of warm ionized gas despite the different accretion rates.

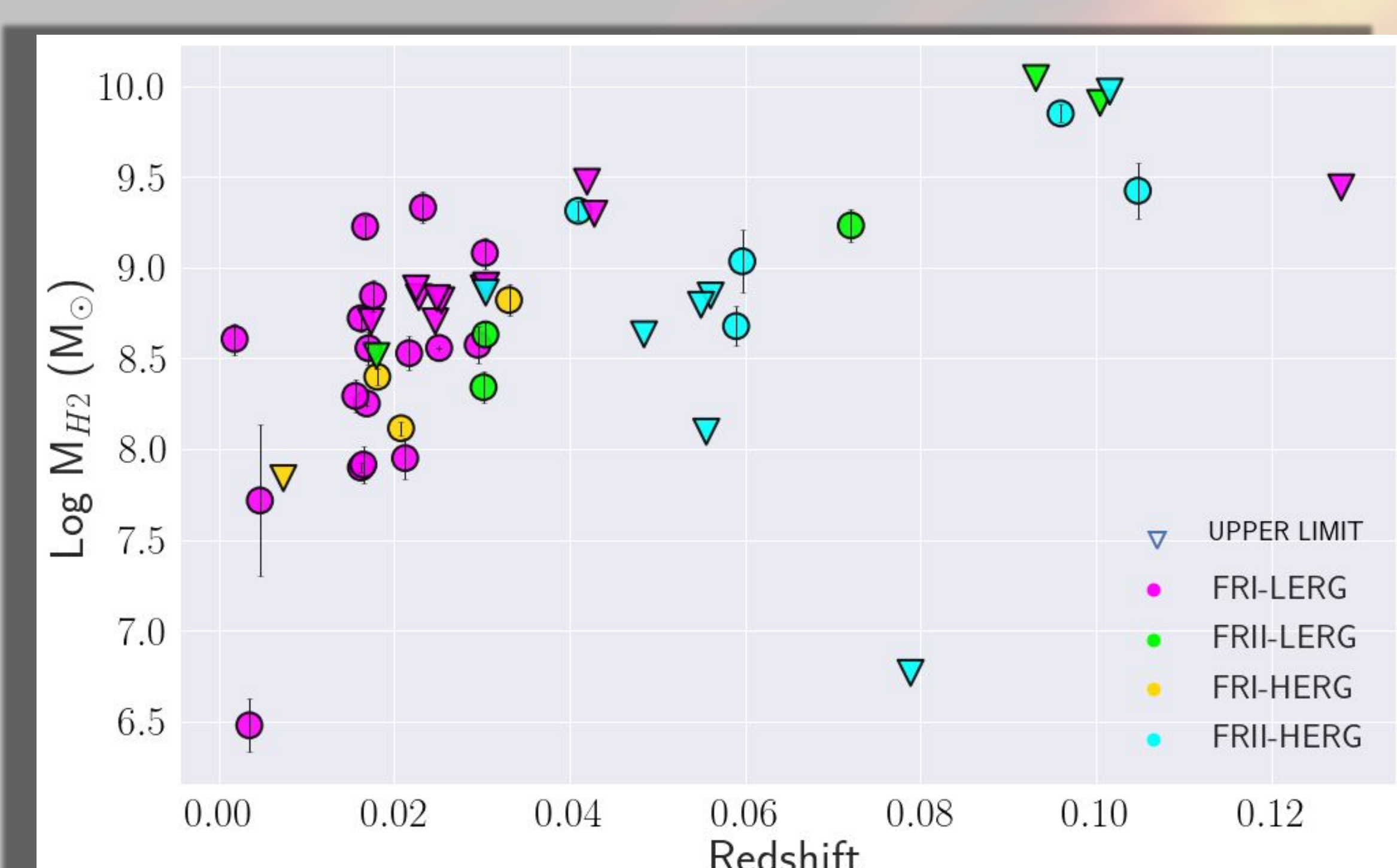


FIG. 4. Molecular gas mass versus redshift for the sources of the sample. Sources at higher redshift tend to have higher molecular gas masses, as it was already pointed out by OF10.

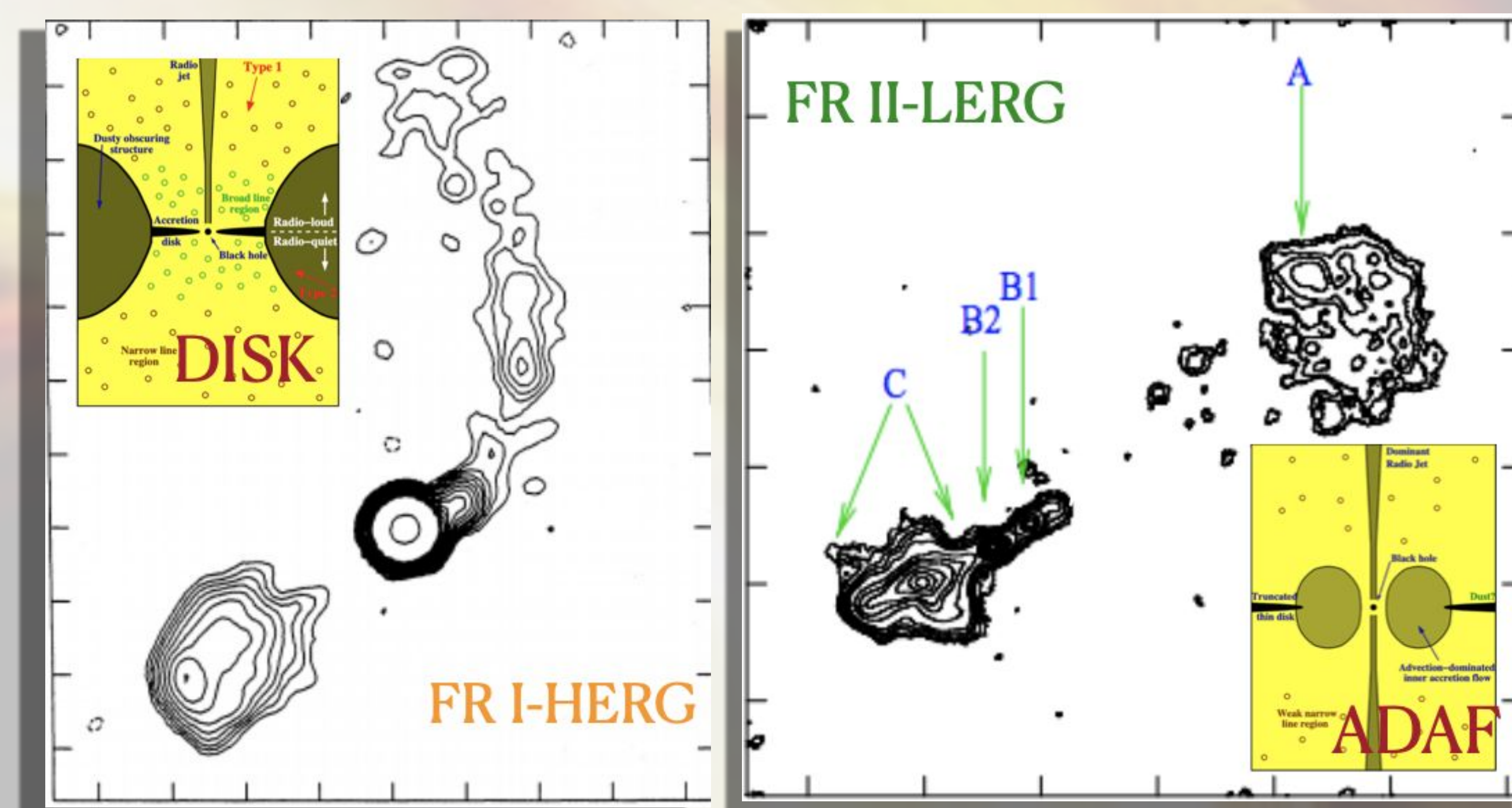


FIG. 1. Example of a FR I-HERG source, i.e., 3C 120 (left panel) and FR II-LERG source, i.e., 3C 236 (right panel).

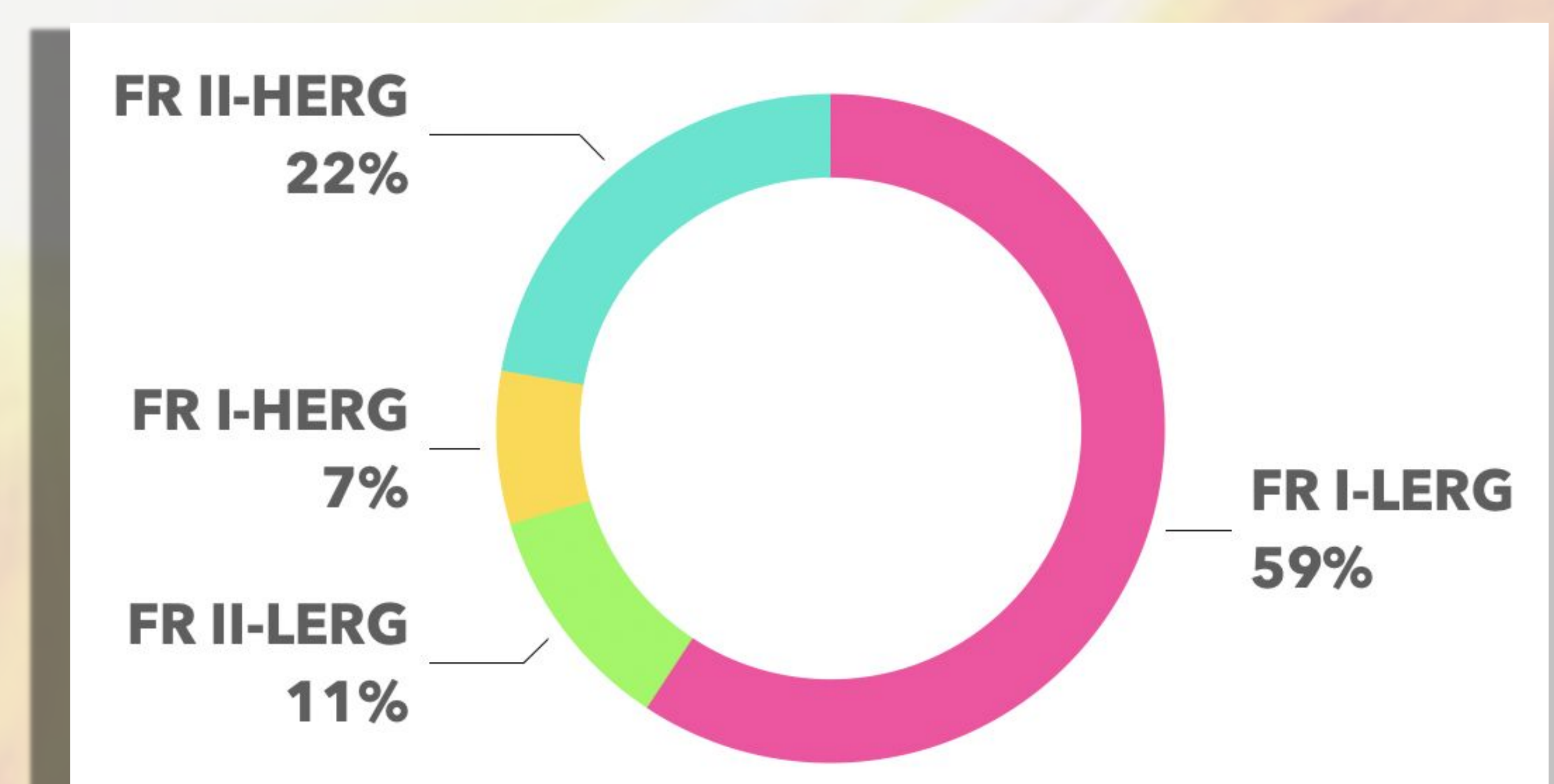


FIG. 2. Fraction of the four classes of radio galaxies (FR I-LERG, FR II-LERG, FR I-HERG and FR II-HERG) considered in the present sample.

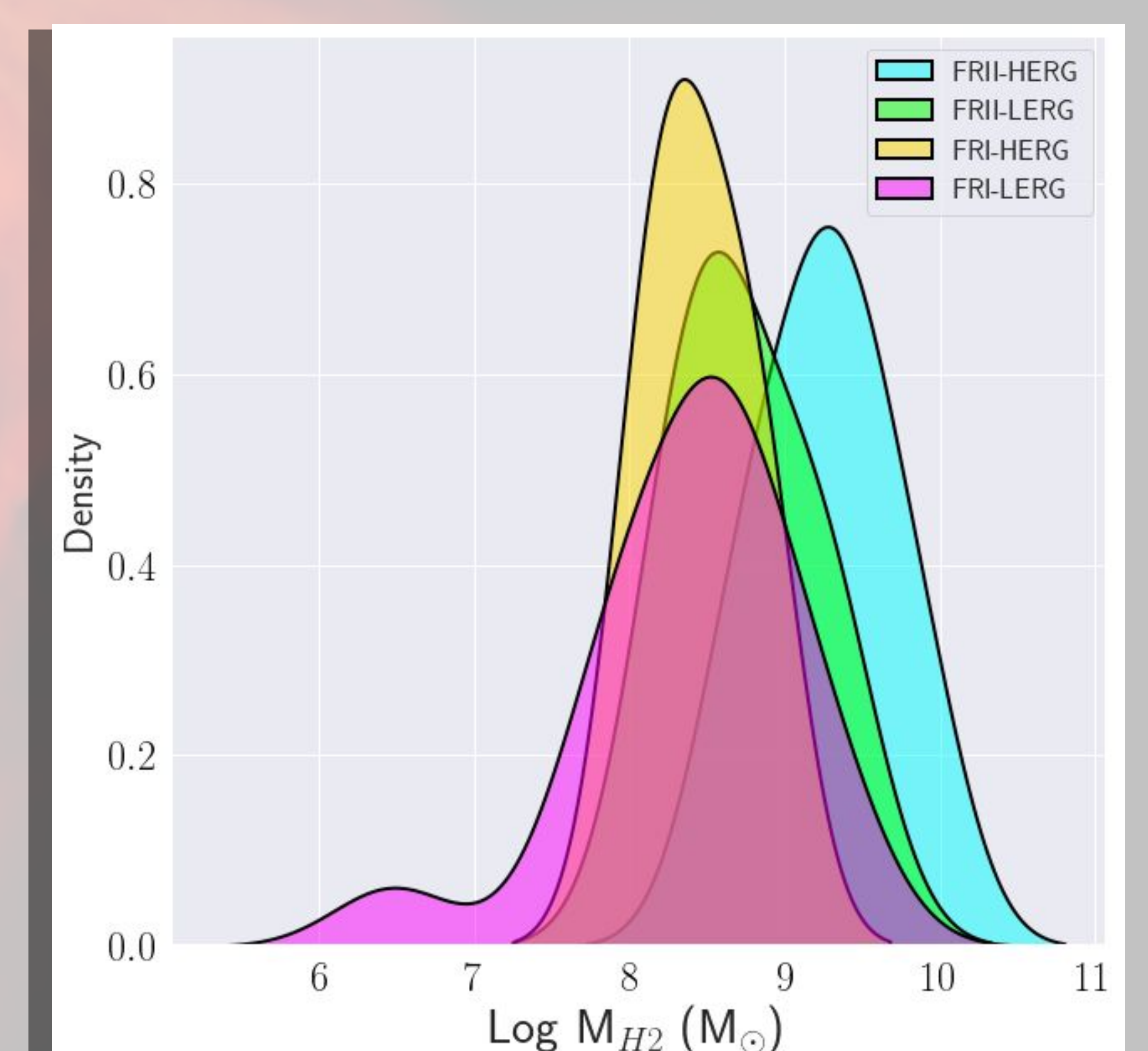


FIG. 3. Kernel density estimation (KDE) of the molecular gas mass for the different classes of radio galaxies (FR I-LERG, FR II-LERG, FR I-HERG, FR II-HERG). While an histogram uses discrete bins, a KDE plot smooths the observations with a Gaussian kernel, producing a continuous density estimate.

BIBLIOGRAPHY

M20 - Macconi, D., Torresi, E., Grandi, P., Boccardi, B., & Vignali, C. 2020, MNRAS, 493, 4355; FR74 - Fanaroff, B. L. & Riley, J. M. 1974, MNRAS, 167, 31P; L94 - Laing, R. A., Jenkins, C. R., Wall, J. V., & Unger, S. W. 1994, in Astronomical Society of the Pacific Conference Series, Vol. 54, The Physics of Active Galaxies, ed. G. V. Bicknell, M. A. Dopita, & P. J. Quinn, 201; JR97 - Jackson, N. & Rawlings, S. 1997, MNRAS, 286, 241; B10 - Buttiglione, S., Capetti, A., Celotti, A., et al. 2010, A&A, 509, A6; GC01 - Ghisellini, G. & Celotti, A. 2001, A&A, 379, L1; S85 - Spinrad H., Djorgovski S., Marr J., Aguilar L., 1985, Publications of the Astronomical Society of the Pacific, 97, 932; OF10 - Ocana-Flaquer, B., Leon, S., Combes, F., & Lim, J. 2010, A&A, 518, A9; E05 - Evans, A. S., Mazzarella, J. M., Surace, J. A., et al. 2005, ApJS, 159, 197; SR11 - Smolcic, V. & Riechers, D. A. 2011, ApJ, 730, 64; L01 - Leon, S., Lim, J., Combes, F., & van-Trung, D. 2001, in QSO Hosts and Their Environments, ed. I. Marquez, J. Masegosa, A. del Olmo, L. Lara, E. Garcia, & J. Molina, 185. <https://arxiv.org/abs/astro-ph/0107498>; G13 - Gendre, M. A., Best, P. N., Wall, J. V., & Ker, L. M. 2013, MNRAS, 430, 3086; FN85 - Feigelson, E.D. & Nelson, P.I. 1985, ApJ, 293, 192; B19 - Balmaverde, B., Capetti, A., Marconi, A., et al. 2019, A&A, 632, A124